Impact of lepton-flavor violating Z' bosons on muon $g-2$ and other muon observables

Brandon Murakami
Department of Physics, Davis Institute for High Energy Physics, University of California, One Shields Avenue, Davis, California 95616
(Received 15 October 2001; published 28 January 2002)

A lepton-flavor violating (LFV) Z' boson may mimic some of the phenomena usually attributed to supersymmetric theories. Using a conservative model of LFV Z' bosons, the recent BNL E821 muon $g-2$ deviation allows for a LFV Z' interpretation with a boson mass up to 4.8 TeV while staying within limits set by muon conversion: $\mu\rightarrow e\gamma$ and $\mu\rightarrow eee$. This model is immediately testable as one to twenty $e^+e^-\rightarrow\mu\tau$ events are predicted for an analysis of the CERN LEP II data. Future muon conversion experiments, MECO and PRIME, are demonstrated to have the potential to probe very high boson masses with very small charges, such as a 10-TeV boson with an e-μ charge of 10^{-5}. Furthermore, the next linear collider is shown to be highly complementary with muon conversion experiments, which are shown to provide the strictest and most relevant bounds on LFV phenomena.

DOI: 10.1103/PhysRevD.65.055003 PACS number(s): 12.10.Dm, 13.10.+q

I. MOTIVATION

When surveying the possibilities for a fundamental theory of nature, extra U(1) gauge symmetries and their quanta, generically dubbed Z' bosons, are often found to exist naturally in the best of the current extensions of the standard model (SM). A renewed interest is urged by recent and future experiments, including the BNL E821 muon anomalous magnetic moment 2.6σ deviation [1], the forthcoming muon conversion experiments MECO and PRIME [2,3]; the Fermilab Tevatron and CERN Large Hadron Collider (LHC), and an anticipated future linear collider. Theoretically, we know of the following sources for Z' bosons:

(i) The implied crossing of the three standard model gauge couplings strongly hints at gauge coupling unification at some high-energy scale. Theories including such unification [grand unified theories (GUTs)] will, in general, include non-SM Z' gauge bosons.

(ii) Theories with compactified extra spatial dimensions [4,5] provide many theoretical tools: a new interpretation of the gauge hierarchy problem, electroweak symmetry-breaking alternative mechanisms [6], and supersymmetry-breaking alternative mechanisms [7]. The photon, SM Z boson, or other neutral vector bosons may form standing waves in the compactified extra dimension. While these excited states may or may not be derived from new gauge symmetries, they will qualitatively mimic Z' phenomenology.

(iii) Supersymmetry is a highly motivated extension of the SM [8,9]. Among a long list, a supersymmetric SM stabilizes the hierarchy problem, explains electroweak symmetry breaking, naturally provides a cold dark matter candidate, and provides a structure that permits baron asymmetry solutions. Particle multiplets in supersymmetric SM theories with $N>1$ will include additional vector bosons.

(iv) String theory is a candidate for a quantum theory of gravity. Supersymmetry and compactified extra dimensions may arise naturally in some string models. If the SM is imbedded within a string model, large gauge groups, such as $E_8\times E_8$ or SO(32), are often required.

(v) Strongly coupled theories provide a dynamical electroweak symmetry-breaking mechanism, eliminate the need for scalar fields (considered unnatural by some), and stabilize the weak scale from renormalizing to the Planck mass [10]. Through the extended gauge structure at the heart of strongly coupled theories, extra Z' gauge bosons may emerge.

Historically, flavor-conserving Z' bosons have been extensively studied, while less attention has been given to the more general case of Z' bosons as a primal source of flavor-changing neutral currents (FCNC). With proper respect for the discovery potential of the forthcoming muon conversion experiments, we focus this paper only on the Z' boson with lepton-flavor violation (LFV) at its primitive vertices. It is feasible that any of the above higher theories will yield a LFV Z' through sufficient model building and interest. In some cases, they already exist in the string models of Refs. [11–13], technicolor models of Refs. [14,15], and the top-flavor model [16]. Because there is no general reason why the grander theories above should supply flavor-conserving Z' bosons, the plausibility of LFV Z' bosons is inherited from the motivations of such models.

Further motivation stems from the strong possibility of detection of weak-scale supersymmetric particles at near-future collider experiments. A supersymmetric analysis of collider signals may be drastically altered by low-scale Z' bosons by providing additional process channels. We demonstrate examples of this by showing how a LFV Z' boson may fully account for any deviations found in lepton anomalous magnetic moments, muon conversion, $\mu\rightarrow e\gamma$, and $\mu\rightarrow eee$.

II. CHOICE OF MODEL

The most general model of an electrically neutral Z' boson would include in its Lagrangian (i) its kinetic term; (ii) fermion interactions $g_{Z'}/\sin\theta_W[\bar{\psi}_i\gamma^\mu(P_L Q_{ij}^{\psi_L}+P_R Q_{ij}^{\psi_R})\psi'_j]Z'_\mu$, (iii) a Higgs sector as a source for the Z' mass, (iv) a non-SM fermion sector necessary to cancel the chiral anomalies of the Z', (v) vector boson interactions, including mass mixing with the Z and other U(1) bosons, and (vi) kinetic mixing terms with other vector bosons [i.e., $(\chi/2)Z^{\mu\nu}Z'_{\mu\nu}$]. The coupling constant is chosen to have $\sin\theta_W$ separated out

to make comparisons to the SM Z boson easier. ψ and ψ' are labels for leptons, up-type quarks, and down-type quarks: $\psi \in \{l,u,d\}$. The subscript on ψ_i refers to flavor. These charges must form symmetric matrices if the Lagrangian is to be Hermitian.

We choose a conservative model, meaning as few parameters as possible while maintaining generic features that should be inherent in any LFV Z' boson. We dub our choice of parameters ''model X,'' and the Z' boson shares the same name, X^μ. To be minimal, effects from the new Higgs and fermion sectors are considered negligible, though their phenomena may be very rich in general. The χ parameter of gauge kinetic mixing is shown to be on the orders of $|\chi|^2 = 10^{-16}$ for gauge-mediated supersymmetry breaking and 10^{-6} for gravity-mediated supersymmetry breaking [17]. Relative to the dominant diagrams for any process considered here, inclusion of kinetic mixing would suppress the contribution by $|\chi|^2$. There is no kinetic mixing in model X; we set $\chi = 0$. Another source of mixing would exist if the SM Z boson and X boson shared a common Higgs mechanism. The physical states observed would then be a quantum admixture, parametrized by a mixing angle θ. The physical Z boson would then inherit some LFV couplings. No mixing is used in model X; $\theta = 0$.

We choose purely vectorial interactions for all fermions with the X boson and drop the helicity subscripts on the charges while setting $Q^{\psi_L} = Q^{\psi_R}$. Separate charges for left- and right-handed vector interactions offer no potential to change phenomenology since spin-averaged observables will contain $|Q_{ij}^{\psi_L}|^2 + |Q_{ij}^{\psi_R}|^2$, which is better off mapped to a single vectorial coupling. A similar mapping can be made for other choices, i.e., purely axial, purely left-handed, etc. However, in purely left- or right-handed interactions, processes that require a helicity flip (i.e., mass insertions) will result in zero for an observable and may be useful for restricting the classes of experiments that may constrain a model, as in Ref. [18]. For non-spin-averaged observables, such as muon $g-2$, more general coupling choices may slightly alter phenomenology; Ref. [19] found muon $g-2$ compatibility at 2σ for the case of purely vectorial couplings, but no compatibility at 2σ for the case of purely axial couplings.

As our focus is LFV, we remove FCNC quark interactions by setting the quark charge matrices to identity, $Q^u = Q^d = 1$. It assumed that the higher theories that provide our X boson present all fermions in the gauge basis of X, in general different from the basis of the SM (ordinary quarks and leptons) with the Yukawa couplings in a nondiagonal basis. The higher theory supplies the X charges in diagonal matrices q^ψ (helicity label omitted). Through unitary matrices U^ψ, the original fermions ψ' are rotated to the SM basis $\psi = U^\psi \psi'$. As a result, the X charges are transformed from q^ψ to $Q^\psi = U^{\psi\dagger} q U^\psi$. The notation for fermion-vector boson interactions is

$$\mathcal{L} \supset \frac{g_X}{\sin\theta_W}[\bar{\psi}_i' q_{ij}^{\psi'} \gamma^\mu \psi_j'] X_\mu = \frac{g_X}{\sin\theta_W}[\bar{\psi}_i Q_{ij}^{\psi} \gamma^\mu \psi_j] X_\mu . \tag{1}$$

We will refer to the Q_{ij} as ''charges'' even though they are not the eigenvalues of a gauge group generator, but rather a simple renaming of the quantity $[U^\dagger q U]_{ij}$.

The charges for the leptons Q_{ij}^l contain the LFV content. For the lepton charges, q^l is chosen to be the diagonal matrix $q^l = \mathrm{diag}(q_{11}^l, q_{11}^l, q_{33}^l)$ with the first two generations sharing the same charge but different from the third generation. This is chosen for two reasons. From the fermion masses, one suspects there to be something special about the third generation and allowing the first two generations to have unique charges does not affect generic behavior in any qualitative way.

All Yukawa unitary rotation matrices are set to the identity matrix except the following two. $U^{u_L} = V_{\mathrm{CKM}}$ is necessary to meet the definition of the Cabibbo-Kobayashi-Maskawa (CKM) matrix. For the lepton charges, a nontrivial U^l will create off-diagonal elements from the diagonal q^l matrix provided q^l is not proportional to the identity matrix. U^l is chosen to borrow the parametrized form of the CKM matrix,

$$U^l = \begin{pmatrix} c_{12}c_{13} & s_{12}c_{13} & s_{13} \\ -s_{12}c_{23} - c_{12}s_{23}s_{13} & c_{12}c_{23} - s_{12}s_{23}s_{13} & s_{23}c_{13} \\ s_{12}s_{23} - c_{12}c_{23}s_{13} & c_{12}s_{23} - s_{12}c_{23}s_{13} & c_{23}c_{13} \end{pmatrix}. \tag{2}$$

The notation s_{ij} and c_{ij} means sines and cosines of parameters $\theta_{12}, \theta_{23}, \theta_{13}$ which need not be the CKM values. We have ignored the allowed complex phase for simplicity. In summary, model X is defined by parameters q_{11}^l, q_{33}^l, three angles for the unitary transformation U^l, the coupling constant g_X, and the boson mass m_X.

III. EXPERIMENTAL CONSTRAINTS ON LFV

Although it is known that LFV may occur in other models such as slepton loops in a supersymmetric SM, loops with neutrino mixing, and other exotic models [20], it assumed that the X boson is the dominant component of LFV effects in the following analysis. With neutrino mixing recently verified to 3σ for active and sterile neutrino models [21,22], LFV is a reality. But to what extent? It can be shown that LFV through neutrino mixing cannot account for any LFV signals found with the sensitivity levels of the future muon conversion experiments. However, a supersymmetric SM enhances LFV effects of neutrino mixing in seesaw mechanisms through Yukawa vertices of the type $H^\pm - l^\mp - \nu$ [23].

Table I lists the experiments considered and the charges they probe at lowest perturbative order. Note that, in general, they all probe different charges. Since all measurements have null results except for the muon anomalous magnetic moment, we may consider two cases, namely the case in which the X boson contributes to the muon anomalous magnetic moment, but does not dominate, and the case in which it does dominate. The reason for this division is due to the great difference in available parameter space between the two cases, the latter case being highly constrained.

In general, for model X, a single experiment from Table I has its charges constrained by any other experiment listed in

TABLE I. The charges listed are only those involved at lowest order. Those in parentheses are involved in diagrams of the same order, but suppressed by either a mass insertion or the charge expected to be small. The quantity R is defined as $\sigma(\mu N \to eN)/\sigma(\mu N \to \nu_\mu N)$ for muon conversion and as the branching ratios for the rare muon decays.

Experiment type	Charges probed	Best measurement
muon $g-2$	$Q^l_{23}(Q^l_{21}, Q^l_{22})$	$\delta a_\mu = (43 \pm 16) \times 10^{-10}$
$\mu N \to eN$	Q^l_{12}	$R < 6.1 \times 10^{-13}$
$\mu \to eee$	Q^l_{11}, Q^l_{12}	$R < 1.0 \times 10^{-12}$
$\mu \to e\gamma$	Q^l_{13}, Q^l_{23} (and all others)	$R < 1.2 \times 10^{-11}$
$e^+e^- \to \mu\tau$	$Q^l_{11}, Q^l_{23}(Q^l_{12} Q^l_{13})$	n/a
$e^+e^- \to \mu^+\mu^-$	$Q^l_{11}, Q^l_{22}(Q^l_{12})$	n/a

Table I. For example, $\mu \to eee$ shares at least one charge in common as $e^+e^- \to \mu\tau$ and muon conversion, $e^+e^- \to \mu\tau$ shares at least one charge in common with a few other experiments, and so on until all six charges are included. There are exceptions to this general feature of model X. This arises when a parameter choice sets one or more charges Q^l_{ij} to zero, such as the universal or generation-dependent Z' cases of model X. For example, setting $Q^l_{12} = 0$ unconstrains a model X interpretation of muon $g-2$ from the strict muon conversion and $\mu \to e\gamma$ limits.

A. The muon anomalous magnetic moment

The X boson participates in the (anti)muon anomalous magnetic moment via a loop involving all charged leptons (Fig. 1). The X boson contribution is dominated by the diagram that includes an internal tau line. This can be seen by noting the two internal tau propagators provide a term proportional to m_τ^2 in the numerator. This dependence is not canceled by the m_τ^2 in the denominator since a heavy X boson mass will dominate the denominator. Therefore, we ignore all other contributions by the X boson and only the μ-τ charge Q^l_{23} is probed. In the limit $m_X \gg m_\tau$, the deviation of the muon anomalous magnetic moment $a_\mu \equiv (g-2)/2$ from the SM value is

$$\delta a_\mu = \frac{g_X^2 (Q^l_{23})^2}{4\pi^2 \sin^2\theta_W} \frac{m_\mu m_\tau}{m_X^2} \tag{3}$$

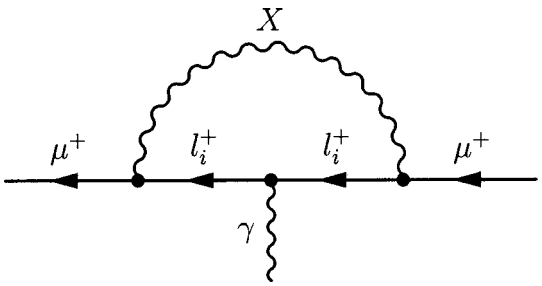

FIG. 1. The leading contributions of a LFV Z' boson to the muon anomalous magnetic moment. The diagram with an internal tau propagator is dominant due to m_τ^2 enhancement in the $g-2$ observable.

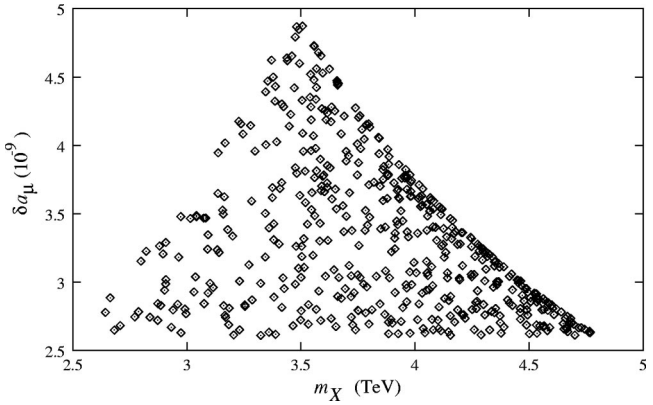

FIG. 2. A scatter plot of the LFV boson mass m_X (TeV) vs the muon anomalous magnetic moment deviation δa_μ. Each point is a point in the parameter space of a LFV Z' boson theory that fully accounts for the BNL E821 muon $g-2$ observed deviation. All points are within limits set by the LFV experiments of Table I, with muon conversion as the strictest limit. ($\nu_\mu e \to \nu_\mu e$ elastic scattering limits are not applied.) The coupling constant is set to the maximal value that retains the perturbative calculation's validity, $g_X/\sin\theta_W = \sqrt{4\pi}$. This is to demonstrate the highest allowed boson mass.

and is measured to be $(43 \pm 16) \times 10^{-10}$ by BNL experiment E821 (2000). Parameter space for model X to account for δa_μ exists but is small when enforcing limits from the LFV experiments listed in Table I. This is accomplished by large μ-τ charge Q^l_{23}, small e-μ charge Q^l_{12}, and relatively small m_X. The boson mass m_X must be balanced between being light enough to account for δa_μ and heavy enough to avoid being ruled out at muon conversion and $\mu \to eee$ experiments. The small Q^l_{12} criterion is required to keep under the same limits. To create a large Q^l_{23}, the special case of $q^l = \mathrm{diag}(-1,-1,1)$ is used since all off-diagonal charges are proportional to the difference in q^l_{11} and q^l_{33} in model X,

$$Q^l_{ij} = (q^l_{33} - q^l_{11}) U^{l\dagger}_{i3} U^l_{3j} \quad (i \neq j). \tag{4}$$

Parameter space compatible with the BNL E821 deviation is tightly bunched around a particular charge assignment,

$$Q^l \approx \begin{pmatrix} -1 & O(10^{-5}) & O(10^{-5}) \\ & 0.1 \text{ to } 1 & 0.4 \text{ to } 1 \\ & & 0.1 \text{ to } 1 \end{pmatrix}. \tag{5}$$

All entries above are magnitudes only. However, a quirk of model X requires the Q^l_{11} entry to be fixed at -1 at its muon $g-2$ optimal compatible value, despite whether or not the case $q^l = \mathrm{diag}(-1,-1,1)$ is used. This parameter space yields an upper limit on the boson mass of $m_X \approx 1$ TeV for $g_X = g_Y$ and $2.8 \lesssim m_X \lesssim 4.8$ TeV for $g_X/\sin\theta_W = \sqrt{4\pi}$, as seen in Fig. 2. $\sqrt{4\pi}$ is chosen to be the highest value of the coupling constant chosen such that next leading order in the perturbative expansion remains smaller than the leading-order contribution. If the constraint $q^l = \mathrm{diag}(-1,-1,1)$ is relaxed, the effect is to widen the range of allowed boson masses.

Q^l_{11} fixed at -1 has the potential to conflict with measurements of elastic scattering of muon neutrinos and electrons,

$\nu_\mu e \to \nu_\mu e$. While not a charge involved in the lowest-order X contribution to muon $g-2$, Q^l_{11} is nonetheless constrained due to the parametrization choice of model X. To examine this constraint, the four-point effective Lagrangian is constructed from the X exchange in the t channel,

$$\mathcal{L}_{\text{effective}} \supset \frac{g_X^2 |Q^l_{11}|^2/\sin^2\theta_W}{t-m_X^2}[\bar{\nu}_\mu \gamma^\lambda P_L \nu_\mu][\bar{e}\gamma_\lambda e], \quad (6)$$

where $P_L=(1-\gamma^5)/2$. This is done for the sake of comparison with the convention of the Particle Data Group (PDG) [Eq. (10.12) of Ref. [24]],

$$\mathcal{L}^{\nu e} = \frac{G_F}{2}[\bar{\nu}_\mu \gamma^\lambda (1-\gamma^5)\nu_\mu][\bar{e}\gamma_\lambda (g_V^{\nu e} - g_A^{\nu e}\gamma^5)e]. \quad (7)$$

This constrains $|Q^l_{11}|$ to $g_V^{\nu e}$. Using a typical momentum transfer value $|t| \ll m_X^2$ and the PDG quoted value of $g_V^{\nu e} = (-0.041 \pm 0.015)$, it is seen that there is no model X parameter space (namely Q^l_{11}) that simultaneously satisfies the muon $g-2$ deviation, muon LFV experiments, and $\nu_\mu e \to \nu_\mu e$ scattering measurements. Therefore, in order for a LFV Z' model to have compatibility with all such data, a modified model X would require either one more additional parameter to unconstrain Q^l_{11} or arbitrarily small couplings to the muon neutrino.

Compatibility without $\nu_\mu e \to \nu_\mu e$ constraints is in agreement with Ref. [25], which uses a submodel of model X to demonstrate a LFV Z' interpretation of the muon $g-2$ deviation. However, the model of Ref. [25] has the limitation of not being able to be tested at a linear collider since it does not include electron couplings (i.e., $Q^l_{11}=0$). Another recent study [26] also utilized submodels of model X (noncommuting extended technicolor and top assisted technicolor), but such models found only small LFV Z' contributions to the muon $g-2$ deviation.

In the case of diagonal charges in Q^l, model X becomes a universal or generation-dependent Z' study. Such models still may account for the muon $g-2$ deviation simply by having a large coupling to the muon. The internal fermion propagator is a muon, and the muon $g-2$ deviation is then

$$\delta a_\mu = \frac{g_X^2 (Q^l_{22})^2}{12\pi^2 \sin^2\theta_W}\frac{m_\mu^2}{m_X^2}, \quad (8)$$

in the limit $m_X \gg m_\mu$. Using $g_X/\sin^2\theta_W = \sqrt{4\pi}$ and $|Q^l_{22}| = 1$, a 660 GeV boson is allowed. With a more familiar value for the coupling constant, $g_X = g_Y$, the boson mass would have to be under 140 GeV to explain the deviation. Neither constraints from CERN e^+e^- collider LEP II and $\nu_\mu e \to \nu_\mu e$ (both probes of Q^l_{11}) may rule out these mass limits due to the possible parameter space in which the electron charge Q^l_{11} can be set arbitrarily small while the muon charge Q^l_{22} is arbitrary. For example, this is seen by the choice that $q^l = \text{diag}(0,0,q^l_{33})$ while the unitary rotations are constrained to $\theta_{12} = \theta_{13} = \pi/2$ with θ_{23} left arbitrary. This results in $Q^l_{11}=0$ and arbitrary Q^l_{22}.

B. $e^+e^- \to \mu\tau$

With the LFV X boson interpretation of the muon $g-2$ deviation requiring a large off-diagonal charge Q^l_{23}, one immediately wonders if model X predicts $e^+e^- \to \mu\tau$ events observed at LEP II. This cross section is

$$\sigma(e^+e^- \to \mu\tau) = \frac{g_X^4}{12\pi \sin^4\theta_W}(Q^l_{11}Q^l_{23})^2 \frac{s}{(s-m_X)^2}. \quad (9)$$

Using a center-of-mass energy of 210 GeV and a total luminosity of 230 pb^{-1}, all parameter space points in the plots of Fig. 2 predict one to about twenty events at LEP II, regardless of the coupling constant g_X. This is fascinating and suggests that an analysis of the LEP II data would be elucidating. If no events are found at LEP II, model X is still a plausible interpretation for the muon $g-2$ deviation since an ample fraction of the parameter space points yields only a handful of events.

Considering $e^+e^- \to e\mu$ is pointless in the foreseeable future due to the strict muon conversion limits. $e^+e^- \to e\tau$ is unmotivated in this study as there is no reason to believe the e-τ charge Q^l_{13} is large. If a LFV Z' is not involved in the dominant contribution to the muon $g-2$ discrepancy, Q^l_{13} may be large but still unmotivated.

C. Muon conversion

Muon conversion is the process $\mu^- N \to e^- N$. Slow negative muons are aimed at a nuclear sample where ground-state muonic atoms are allowed to form. The muon eventually undergoes SM decay in which a W boson is emitted from the muon towards the nuclei or outside the atom. The ratio of muon conversion to weak decays is defined as $R(\mu N \to eN) \equiv \sigma(\mu N \to eN)/\sigma(\mu N \to \nu_\mu N')$. SINDRUM II at the Paul Scherrer Institut (PSI) holds the current best limit of 6.1×10^{-13} (1998) [27]. MECO (muon electron conversion) at Brookhaven (E940) may collect data in 2006 with a sensitivity of 2×10^{-16} [28]. PRIME (prism mu-e conversion) will use the PRISM high-intensity muon source at the Japan Hadron Facility (to be renamed) at KEK and may collect data in 2007 with a sensitivity of 10^{-18} [29]. This great technological leap of more than four orders of magnitude warrants LFV as a larger part of our community's consciousness for the next decade.

The muon conversion ratio is [30]

$$R(\mu N \to eN)$$

$$= \frac{G_F^2 \alpha^3 m_\mu^5}{2\pi^2 \Gamma_{\text{capture}}}\frac{Z_{\text{eff}}^4}{Z}|F_P|^2(|Q^{l_L}_{12}|^2 + |Q^{l_R}_{12}|^2)$$
$$\times\left|\frac{g_X}{g_Y}\sin\theta\cos\theta\left(1-\frac{m_W^2}{m_X^2\cos^2\theta_W}\right)\right|[\tfrac{1}{2}(Z-N)$$
$$-2Z\sin^2\theta_W] + \frac{g_X^2}{g_Y^2}\left(\sin^2\theta + \frac{m_W^2}{m_X^2\cos^2\theta_W}\cos^2\theta\right)$$
$$\times[(2Z+N)(|Q^{u_L}_{11}|^2 + |Q^{u_R}_{11}|^2) + (Z+2N)(|Q^{d_L}_{11}|^2$$

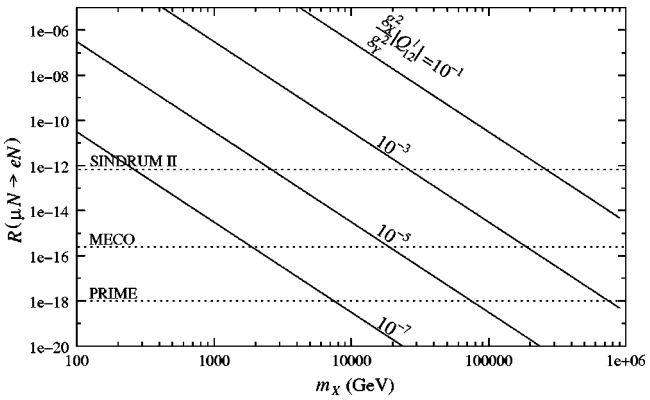

FIG. 3. LFV boson mass m_X (GeV) vs the muon conversion rate $R(\mu^- N \to e^- N)$. This plot demonstrates the discovery potential of future muon conversion experiments. The diagonal lines represent different values of the μeX vertex coupling. Note the surprisingly large boson mass and small couplings accessible by future experiments MECO and PRIME. This plot does not assume the LFV should account for all of the BNL E821 muon $g-2$ observed deviation.

$$+|Q_{11}^{d_R}|^2)]\Bigg|^2. \tag{10}$$

Using ^{48}Ti as the sample, the nuclear form factor $F_P=0.54$ [31], $Z_{\text{eff}}=17.6$ [32], and the muon capture rate $\Gamma_{\text{capture}}=2.6\times10^{-6}$ s^{-1} [33]. In model X, this simplifies to

$$R(\mu N\to eN)=3.1\times10^{-11}\left(\frac{g_X}{g_Y}\right)^4\left(\frac{Q_{12}^l}{10^{-5}}\right)^2\left(\frac{1\text{ TeV}}{m_X}\right)^4. \tag{11}$$

Note that $R\propto 1/m_X^4$ means for every four orders of magnitude gained through the experimentalists' efforts, it becomes possible to probe Z' bosons exactly one magnitude more massive. All processes that involve only one Z' internal propagator will share this feature in its observable, such as $\mu\to eee$ and $\mu\to e\gamma$.

The vast discovery potential of future muon conversion experiments is demonstrated in Fig. 3. This plot and all plots to follow do not assume that the model X boson fully accounts for the muon $g-2$ observed deviation. Figure 3 is best appreciated by noting the large boson masses and small e-μ charges Q_{12}^l accessible. For example, a LFV signal at PRIME may imply a model X boson with a mass about $O(10\text{ TeV})$ and couplings as small as $O(10^{-5})$. Even without a LFV signal, MECO and PRIME will provide strict bounds on theoretical models that include LFV.

Due to the stringent current muon conversion limit, Q_{12}^l is constrained to be very small for light X bosons. Because of the relationships between all charges of model X, muon conversion constrains the parameter space of model X more so than any other experiment, as will be shown in the following subsections.

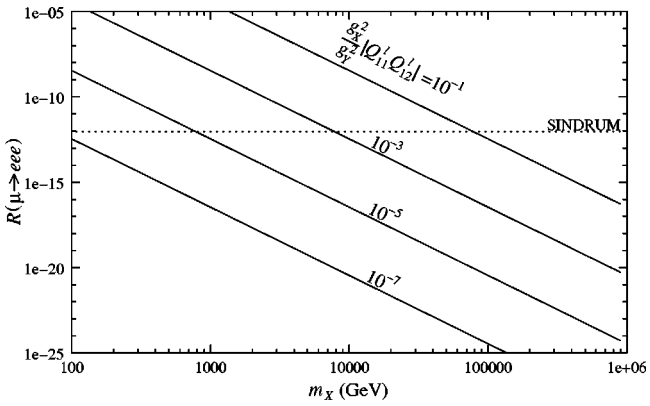

FIG. 4. LFV boson mass m_X (GeV) vs the branching ratio $R(\mu\to eee)$. The value of this plot is understood if compared to Fig. 3. It is obvious that the current limits of muon conversion and $\mu\to eee$ are competitive in their parameter space coverage. More subtle is noting that muon conversion has probed more parameter space than $\mu\to eee$. For example, using $Q_{11}^l=-1$ and $Q_{12}^l=10^{-5}$ (the muon $g-2$ optimal parameters), muon conversion has probed the LFV boson mass to 2 TeV while $\mu\to eee$ probed to 800 GeV. Therefore, in the near future, muon conversion warrants more attention as the MECO and PRIME experiments are coming online in 2006 and 2007, respectively. This plot does not assume the LFV should account for all of the BNL E821 muon $g-2$ observed deviation.

D. $\mu\to eee$

This process has been historically performed using antimuons at rest, $\mu^+\to e^+e^+e^-$. A negative muon will tend to be captured by a nucleus in the target used to stop the muon, and is therefore not used. $\mu\to eee$ is similar to muon conversion in that they both stringently probed the e-μ charge Q_{12}^l. $\mu\to eee$ differs in that it also probes e-e charge Q_{11}^l at tree level.

The partial width for $\mu\to eee$ is

$$\Gamma(\mu\to eee)=\frac{G_F^2m_\mu^5}{4\pi^3}\left(\frac{g_X}{g_Y}\right)^4(Q_{11}^lQ_{12}^l)^2\left(\frac{m_Z}{m_X}\right)^4. \tag{12}$$

The branching ratio for model X at tree level results in

$$R(\mu\to eee)=3.4\times10^{-13}\left(\frac{g_X}{g_Y}\right)^4\left(\frac{Q_{11}^lQ_{12}^l}{10^{-5}}\right)^2\left(\frac{1\text{ TeV}}{m_X}\right)^4. \tag{13}$$

The current sensitivity level is $R(\mu\to eee)<1.0\times10^{-12}$ from SINDRUM at PSI (1988) [34]. There are no major $\mu\to eee$ projects announced as forthcoming. However, with the future high-intensity muon sources in the works, a near-future experiment is still plausible.

Figure 4 shows us that $\mu\to eee$ is a competitive experiment with muon conversion for probing the e-μ charge Q_{12}^l. Closer inspection reveals muon conversion has probed more parameter space than $\mu\to eee$. For example, if the muon $g-2$ parameters of $Q_{11}^l=-1$ and $Q_{12}^l=10^{-5}$ are used, $\mu\to eee$ has probed X bosons to 800 GeV while muon conversion has probed to 2 TeV. Furthermore, muon conversion has

provided stricter bounds than linear and hadronic collider searches for generation-dependent Z' bosons that originate from $SU(2)_h \times SU(2)_l$ and $U(1)_l \times U(1)_h$ extended electroweak gauge structures (special cases of model X), as studied in Refs. [37,38] in which a lower boson mass limit of 375 GeV is claimed.

There are similar processes for the tau lepton: $\tau \rightarrow \mu\mu\mu$, $\tau \rightarrow ee\mu$, $\tau \rightarrow \mu\mu e$, and $\tau \rightarrow eee$. However, the branching ratios for all of these are on the order of $O(10^{-6})$ and place too weak constraints to be of relevance in this study [24].

E. $\mu \rightarrow e\gamma$

$\mu^+ \rightarrow e^+\gamma$ has historically been probed by allowing an antimuon at rest to decay and waiting for back-to-back decay products. For the same reasons as $\mu \rightarrow eee$, a negative muon is not used. The dominant diagrams for $\mu \rightarrow e\gamma$ are identical to the muon $g-2$ with the outgoing antimuon exchanged for a positron. This provides a new probe by changing the charges probed at the vertices involving the positron. In principle, $\mu \rightarrow e\gamma$ probes all charges of model X. However, a tau internal propagator dominates for the same reasons it should dominate lepton anomalous magnetic moments. This effectively reduces the charges probed to only Q^l_{13} and Q^l_{23}.

The partial width for $\mu \rightarrow e\gamma$ is

$$\Gamma(\mu \rightarrow e\gamma) = \frac{\alpha G_F^2}{4\pi^4}\left(\frac{g_X}{g_Y}\right)^4 \frac{m_W^4 m_\mu^3 M_{12}^2}{m_X^4}, \tag{14}$$

where

$$M_{12} = m_e Q^l_{11} Q^l_{12} + m_\mu Q^l_{12} Q^l_{22} + m_\tau Q^l_{13} Q^l_{23}. \tag{15}$$

For model X, the branching ratio results in

$$R(\mu \rightarrow e\gamma) = 1.3 \times 10^{-13}\left(\frac{g_X}{g_Y}\right)^4 \left(\frac{Q^l_{13} Q^l_{23}}{10^{-5}}\right)^2 \left(\frac{1\ \text{TeV}}{m_X}\right)^4. \tag{16}$$

The current limit is held by MEGA at LANL (1999) to be $R(\mu \rightarrow e\gamma) < 1.2 \times 10^{-11}$ [35]. A recently approved experiment MEG at PSI may reach a sensitivity of 10^{-14} [36] in 2003. From Fig. 5, it is seen that the muon conversion limit overrides the $\mu \rightarrow e\gamma$ limit when considering the parameter space covered in model X. For example, using the muon $g-2$ optimal charges again, $|Q^l_{13} Q^l_{23}| = 1$, $\mu \rightarrow e\gamma$ has only probed the model X boson up to about 200 GeV. An earlier effort confirmed this ranking of LFV experiments for topcolor assisted technicolor, a specific case of model X [14].

Because of the relatively weak branching ratio limits for $\tau \rightarrow \mu\gamma$ and $\tau \rightarrow e\gamma$ (both on the order of 10^{-6}), those analyses are rendered irrelevant for model X [24]. However, a stronger limit on $\tau \rightarrow \mu\gamma$ could prove interesting since the charges involved, Q^l_{23} and Q^l_{33}, may have magnitudes near 1 for the muon $g-2$ optimal charges.

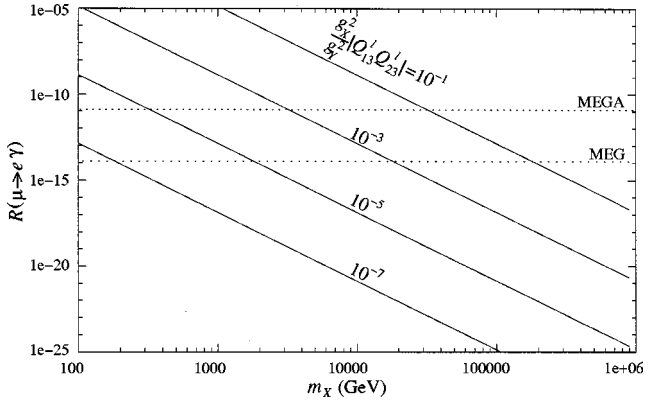

FIG. 5. LFV boson mass m_X (GeV) vs the branching ratio $R(\mu \rightarrow e\gamma)$. It is important to eliminate the possible confusion over which experiments are most constraining for a given model. The value of this plot is in revealing that the $\mu \rightarrow e\gamma$ MEGA limit is of little value to constrain model X bosons beyond or complementary to muon conversion when BNL E821 muon $g-2$ constraints are applied. The muon $g-2$ optimal charges are $|Q^l_{13}Q^l_{23}| = 10^{-5}$, and therefore MEGA has probed model X bosons to about 200 GeV for $g_X = g_Y$. If muon $g-2$ constraints are relaxed, with large e-τ charge Q^l_{13}, the MEGA limit has probed to very large LFV Z' boson masses, i.e., 10 TeV for $(g_X/g_Y)^2|Q^l_{13}Q^l_{23}| = 10^{-2}$. This plot does not assume the LFV should account for all of the muon $g-2$ observed deviation.

F. $e^+e^- \rightarrow \mu^+\mu^-$

$e^+e^- \rightarrow l^+l^-$ is included in our analysis to provide a simple way of constraining the mass of any Z' model at future linear colliders. Because the cross section $\sigma(e^+e^- \rightarrow l^+l^-)$ is insensitive to what outgoing charged lepton is used, we arbitrarily choose muons as outgoing. At tree level, this process is dominated by the s-channel exchange involving only charges Q^l_{ii}. t-channel exchange suffers $(Q^l_{12})^4$ suppression, rendering it relevant only for X bosons with masses somewhere over 1000 TeV, where the e-μ coupling $(g_X/g_Y)^2 Q^l_{12}$ may be 1 or larger (Fig. 3). This would come at the expense of losing a LFV Z' interpretation of the muon $g-2$ observed discrepancy.

The next linear colliders have the potential to show a 1% deviation in the cross section for $e^+e^- \rightarrow l^+l^-$. It is assumed that a 1% observed difference in $\Delta\sigma(e^+e^- \rightarrow \mu^+\mu^-)/\sigma_{SM}(e^+e^- \rightarrow \mu^+\mu^-)$ is entirely due to the X boson. We include interference with photon and Z exchange in $\Delta\sigma$. Figure 6 has the parameter space limits set forth by future linear colliders superimposed with the limits set by muon conversion. Parameters $g_X = g_Y$, $Q^l_{11} = -1$, and $Q^l_{22} = -1$ are used.

It is seen that the future muon conversion and linear collider experiments are highly complementary in their search for a model X boson. Signals implying parameters in the upper left "quadrant" of m_X and Q^l_{12} parameter space can be seen at both types of experiments. The larger masses in the upper left quadrant can be seen only by muon conversion experiments. Due to the insensitivity to t-channel exchange, future linear colliders may probe the region of arbitrarily

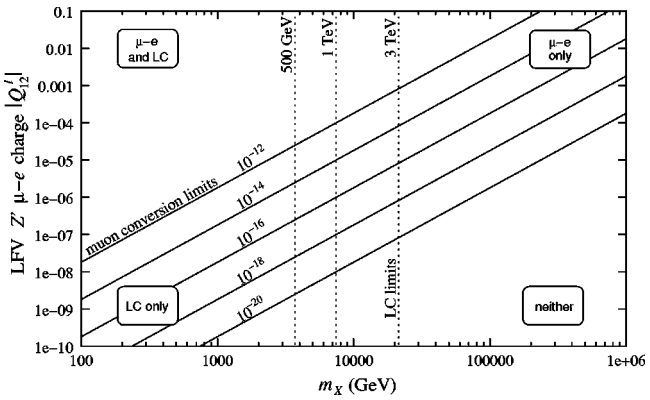

FIG. 6. LFV Z' boson mass m_X (GeV) vs the electron-muon charge Q^l_{12}. This plot demonstrates future muon conversion and linear collider experiments to be highly complementary. The vertical lines show the maximum Z' mass that would show a 1% deviation in $\Delta\sigma(e^+e^-\to\mu^+\mu^-)/\sigma_{\rm SM}(e^+e^-\to\mu^+\mu^-)$ with parameters $g_X=g_Y$, $Q^l_{11}=-1$, and $Q^l_{22}=-1$. The diagonal lines are limits that would be set by future muon conversion experiments. The upper left "quadrant" contains parameter space that would be implied at both types of experiments. The upper right quadrant contains parameters that could only be implied at future muon conversion experiments. The lower left quadrant contains parameters that could only be implied by future linear colliders. Neither type of experiment could see the parameters of the lower right quadrant.

small e-μ charge in the lower left corner. Neither type of experiments will see the lower right corner.

IV. SUMMARY

Theoretical and experimental motivations for a lepton-flavor violating Z' boson are explored. A LFV Z' boson interpretation is applied to recent and near-future experiments. A conservative model was chosen by balancing the least number of free parameters while not sacrificing generic phenomenological behavior. Through this "model X," we established the following.

(i) The BNL E821 muon $g-2$ deviation may fully be attributed to an X boson with a mass as large as roughly 6 TeV, or less as the coupling constant g_X is lowered. This LFV boson will also maintain compatibility with muon conversion, $\mu\to eee$, and $\mu\to e\gamma$ experimental null searches.

(ii) Even without LFV, a Z' with only lepton-flavor conserving interactions may still account for the muon $g-2$ deviation with masses as large as 660 GeV. No linear collider may place a limit on this mass due to the parameter space that allows for arbitrarily small eeX couplings.

(iii) Model X is immediately testable. Nearly all parameter space points in the first claim above will have produced one to twenty $e^+e^-\to\mu\tau$ events at LEP II. An analysis of the LEP II data is therefore urged.

(iv) The technological advances incorporated in future muon conversion experiments, MECO (2006) and PRIME (2007), will improve probes of LFV Z' masses by more than an order of magnitude. For example, 10 TeV bosons with couplings of 10^{-5} will be accessible.

(v) Furthermore, muon conversion places the strictest lower bounds on LFV Z' masses over all other experiments, including $\mu\to eee$, $\mu\to e\gamma$, and all collider searches. MEG, a future $\mu\to e\gamma$ experiment, will not probe model X bosons beyond what muon conversion already has. With no forthcoming $\mu\to eee$ experiments announced, the importance of MECO and PRIME for the next decade is emphasized.

(vi) Future linear colliders will be complementary in their search for Z' bosons. As they are insensitive to LFV primal vertices, linear colliders provide different limits, as explained in Fig. 6.

ACKNOWLEDGMENTS

We thank S. Mrenna, K. Tobe, and J. Wells for helpful discussions. This work was funded in part by the U.S. Department of Energy.

[1] Muon $g-2$ Collaboration, H. N. Brown *et al.*, Phys. Rev. Lett. **86**, 2227 (2001).
[2] http://meco.ps.uci.edu/
[3] http://www-prism.kek.jp/
[4] N. Arkani-Hamed, S. Dimopoulos, and G. Dvali, Phys. Lett. B **429**, 263 (1998).
[5] L. J. Randall and R. Sundrum, Phys. Rev. Lett. **83**, 3370 (1999).
[6] B. A. Dobrescu, Phys. Lett. B **461**, 99 (1999).
[7] A. Delgado, A. Pomarol, and M. Quiros, Phys. Rev. D **60**, 095008 (1999).
[8] H. E. Haber and G. L. Kane, Phys. Rep. **117**, 75 (1985).
[9] S. P. Martin, "A supersymmetry primer," hep-ph/9709356.
[10] K. D. Lane, "Technicolor 2000," hep-ph/0007304.
[11] E. Nardi, Phys. Rev. D **48**, 1240 (1993).
[12] G. B. Cleaver, A. E. Faraggi, D. V. Nanopoulos, and T. ter Veldhuis, Int. J. Mod. Phys. A **16**, 3565 (2001).
[13] S. Chaudhuri, S. Chung, G. Hockney, and J. Lykken, Nucl. Phys. **B456**, 89 (1995).
[14] T. Rador, Phys. Rev. D **59**, 095012 (1999).
[15] C. Yue, G. Liu, and J. Li, Phys. Lett. B **496**, 89 (2000).
[16] D. J. Muller and S. Nandi, Phys. Lett. B **383**, 345 (1996).
[17] K. R. Dienes, C. Kolda, and J. March-Russell, Nucl. Phys. **B492**, 104 (1997).
[18] B. Murakami and J. D. Wells, in the proceedings of the 2001 APS Snowmass Summer Study.
[19] D. Choudhury, B. Mukhopadhyaya, and S. Rakshit, Phys. Lett. B **507**, 219 (2001).
[20] Y. Kuno and Y. Okada, Rev. Mod. Phys. **73**, 151 (2001).
[21] J. N. Bahcall, M. C. Gonzalez-Garcia, and C. Pena-Garay, J. High Energy Phys. **108**, 014 (2001).
[22] V. Barger, D. Marfatia, and K. Whisnant, Phys. Rev. Lett. **88**, 011302 (2002).
[23] J. Hisano and D. Nomura, "Neutrino oscillation and charged lepton flavor violation in the supersymmetric standard models," hep-ph/0004061.
[24] Particle Data Group, D. E. Groom *et al.*, Eur. Phys. J. C **15**, 1 (2000).

[25] T. Huang, Z. H. Lin, L. Y. Shan, and X. Zhang, Phys. Rev. D **64**, 071301(R) (2001).
[26] K. R. Lynch, Phys. Rev. D (to be published), hep-ph/0108080.
[27] P. Wintz, in *Proceedings of the First International Symposium on Lepton and Baryon Number Violation*, edited by A. Astbury, D. Axen, and J. Robinson (World Scientific, Singapore, 1999), p. 534.
[28] W. Molzon (private communication).
[29] Y. Kuno (private communication).
[30] P. Langacker and M. Plumacher, Phys. Rev. D **62**, 013006 (2000).
[31] J. Bernabeu, E. Nardi, and D. Tommasini, Nucl. Phys. **B409**, 69 (1993).
[32] J. C. Sens, Phys. Rev. **113**, 679 (1959).
[33] T. Suzuki, D. F. Measday, and J. P. Roalsvig, Phys. Rev. C **35**, 2212 (1987).
[34] SINDRUM Collaboration, U. Bellgardt *et al.*, Nucl. Phys. **B299**, 1 (1988).
[35] MEGA Collaboration, M. L. Brooks *et al.*, Phys. Rev. Lett. **83**, 1521 (1999).
[36] http://meg.icepp.s.u-tokyo.ac.jp/
[37] K. R. Lynch, E. H. Simmons, M. Narain, and S. Mrenna, Phys. Rev. D **63**, 035006 (2001).
[38] R. S. Chivukula, E. H. Simmons, and J. Terning, Phys. Lett. B **331**, 383 (1994).